Major gradients in putatively nitrifying and non-nitrifying Archaea in the deep North Atlantic

Hélène Agogué, Maaike Brink, Julie Dinasquet, Gerhard J Herndl

Major gradients in putatively nitrifying and non-nitrifying Archaea in the deep North Atlantic

Hélène Agogué, Maaike Brink, Julie Dinasquet and Gerhard J. Herndl

Department of Biological Oceanography, Royal Netherlands Institute for Sea Research (Royal NIOZ), P.O. Box 59, 1790 AB Den Burg, Texel, The Netherlands.

Aerobic nitrification of ammonia to nitrite and nitrate is a key process in the oceanic nitrogen cycling mediated by prokaryotes[1]. Besides the two different groups of Bacteria belonging to the beta- and gamma-proteobacteria involved in the first nitrification step, *Crenarchaeota* have been recently recognized as main drivers of the oxidation of ammonia to nitrite in soil as well as in the ocean as indicated by the dominance of archaeal ammonia monooxygenase (*amo*A) genes over bacterial *amo*A[2,3]. Evidence is accumulating that archaeal *amo*A genes are common in a wide range of marine systems[3-6]. Essentially all these reports focused on surface and mesopelagic (200-1000 m depth) waters where ammonia concentrations are higher than in waters below 1000 m depth. *Crenarchaeota* are abundant, however, also in the water column below 1000 m depth where ammonia concentrations are extremely low. Here we show, that throughout the North Atlantic, the abundance of archaeal *amo*A genes decreases drastically from subsurface waters to 4000 m depth and from the subpolar to the equatorial deep waters leading to pronounced vertical and latitudinal gradients in the ratio of archaeal *amo*A to crenarchaeal 16S rRNA genes. The lack of significant copy numbers of *amo*A genes in combination with the very low dark carbon dioxide fixation rates in the bathypelagic North Atlantic suggests that the vast majority of the bathypelagic *Crenarchaeota* are not autotrophic ammonia oxidizers but most likely utilize organic matter, hence live heterotrophically.

Planktonic Archaea consisting of the two major groups, *Crenarchaeota* and *Euryarchaeota*, might account for about one-third of all prokaryotic cells in the global ocean[7,8]. *Crenarchaeota* are generally more abundant than *Euryarchaeota* in marine waters[7-9] and mainly composed of the Marine *Crenarchaeota* Group I (MCGI) and the deep-branching pSL12-like clade[4]. Until recently, only members the bacterial domain, γ- and β-proteobacteria were known to carry out the oxidation of NH_4^+ to NO_2^- and γ-, β-, δ- proteobacteria and *Nitrospira* species to oxidize the intermediate product NO_2^- to NO_3^- [1]. Recent genomic studies suggest that mesophilic *Crenarchaeota* might play a role in the ammonia oxidation as the *amo*A gene encoding a subunit of one of the key enzymes in the ammonia oxidation, ammonia monooxygenase, has been detected[2,10,11]. The only two mesophilic marine crenarchaeal isolates (i.e., *Cenarchaeum symbiosum* and *Nitrosopumilus maritimus*) carry also this *amo*A gene[12,13]. Recent quantitative studies showed that MCGI oxidize ammonia as their energy source and that archaeal *amo*A genes are, at least, one order of magnitude more abundant than bacterial *amo*A in various marine as well as in soil environments[3-5,14,15]. Moreover, recently, Mincer *et al.* [4] suggested that the pSL12-like clade may also contain *amo*A genes. Taken together, there is evidence that at least some of the MCGI are chemoautotrophic ammonia oxidizers although other studies indicate that *Crenarcheaota* might be heterotrophic as well[8,16-19].

All the studies quantifying archaeal *amo*A gene abundance in the pelagic realm, however, focused on the euphotic and mesopelagic zone where ammonia is generated by remineralisation processes such as in the oxygen minimum zone[3-5,11]. Also the only-free living isolate, *Nitrosopumilus maritimus*, has been obtained from an ammonia-rich tropical aquarium[12]. However, *Crenarchaeota* are abundant in the bathypelagic (1000-4000 m depth) waters as well[20,21] where ammonia concentrations are below 5 nM (M. Woodward, personal communication) and only detectable with highly sensitive methods making it unlikely that ammonia is readily available as an energy source in these deep waters.

The contribution of putatively ammonia-oxidizing Archaea (AOA) and Bacteria (AOB) to the total archaeal and bacterial communities was determined by quantitative PCR (Q-PCR) in the main water masses of the Atlantic from 65°N to 5°S covering a depth range from 100 m to 4000 m. The abundance of specific groups of planktonic *Crenarchaeota* (MCGI and pSL12-like clade) based on 16S rRNA gene fragments was determined and compared with the abundance of AOA and AOB using two specific primer sets targeting archaeal and bacterial *amo*A genes at 10 stations, comprising different water masses with specific physical and chemical characteristics (for details see Supplementary Fig. 1 and Table 1, 2).

Highest MCGI abundance was found in the mesopelagic layer in almost all the stations and particularly in the oxygen minimum layer (i.e., between 200 and 600 m depth) (Fig. 1a, Supplementary Tables 1 and 3). The abundance of the pSL12-like clade was about 1.5 orders of magnitude lower than MCGI (Supplementary Table 3). In most of the samples (40 out of 55), the contribution of the pSL12-like clade to total crenarchaeal abundance was less than 5% (Supplementary Table 3) but followed a similar vertical distribution pattern as MCGI. The pSL12-like clade was more abundant just below the euphotic zone (i.e., 250 m depth) than in deeper water masses (Supplementary Table 3). A similar trend was observed by Mincer *et al.*[4] who found more pSL12-related members below the euphotic zone of the north Pacific subtropical gyre. The distribution of the copy numbers of the 16S rRNA genes (MCGI and pSL12-clade) obtained by Q-PCR corresponds to the distribution pattern of *Crenarchaeota* with depths reported previously using fluorescent in situ hybridization[7,8,20,21]. Overall, marine *Crenarchaeota* seem to be particularly associated with the oxygen minimum zone[4,5,11,22].

Copy numbers of archaeal *amo*A genes were always highest at the base of the euphotic zone ranging from 2.5 x 10^3 to 25 x 10^3 ml^{-1} decreasing with depth (Fig. 1b, Supplementary Table 3). While no latitudinal trend in the abundance of the archaeal

*amo*A genes was detectable at the base of the euphotic zone, in deeper waters, archaeal *amo*A copy numbers decreased by 2-3 orders of magnitude from the subpolar to the subtropical and equatorial Atlantic (Fig. 1b, Supplementary Table 3). The higher abundance of archaeal *amo*A genes in the meso- and bathypelagic waters in the northern part of the Atlantic coincides with the higher ammonia concentrations there[21] as these deep waters have been recently formed and therefore, are younger than in the southern part of the North Atlantic[23]. In contrast to the high number of archaeal *amo*A copy numbers, β-proteobacterial *amo*A copy numbers were at least one order of magnitude lower than archaeal *amo*A gene abundance in the individual depth layers (Supplementary Table 3). Gamma-proteobacterial *amo*A genes were not quantified in this study since ammonia-oxidizing γ-proteobacteria were not detected in this region of the Atlantic by Q-PCR in a previous study[3] nor in Arctic and North Pacific samples[4,24]. Taken together, our data confirm previous findings that the crenarchaeal *amo*A genes are by far more abundant than bacterial *amo*A in marine systems[3,5,15].

The average ratio of archaeal *amo*A copy numbers versus crenarchaeal 16S rRNA genes in the subsurface waters (100-150 m depth) was close to 1, particularly in the northern and equatorial North Atlantic, while it was <0.01 in the bathypelagic waters of the subtropical and equatorial region of the North Atlantic (Fig. 1c, Supplementary Fig. 2). Our ratios for the surface waters are similar to those of Mincer *et al.*[4] reporting a ratio between archaeal *amo*A and archaeal 16S rRNA genes of about 1 while Wuchter *et al.*[3] and Beman *et al.*[5] reported a ratio of 2.8 and 2.5, respectively. Genomic studies on the two mesophilic crenarchaeal isolates obtained thus far revealed that *Cenarchaeum symbiosum* and as well as *Nitrosopumilus maritimus* contain only one *amo*A gene copy per cell[13]. In the 100-150 m depth range, the average ratios between archaeal *amo*A and crenarchaeal 16S rRNA genes were 0.9, 0.4 and 0.7 for the northern, the subtropical and the equatorial region, respectively (Fig. 1c). We conclude therefore, that in subsurface waters most of the *Crenarchaeota* are putatively capable of ammonia oxidation throughout the North

Atlantic. In the northern part of the Atlantic (65°N-30°N), the ratio archaeal *amo*A to crenarchaeal 16S rRNA genes decreased only by about one order of magnitude from the surface waters to the bathypelagic realm (Fig. 1c). In the subtropical and equatorial regions of the Atlantic (30°N-5°S), however, this ratio decreased by at least two orders of magnitude from the subsurface to the bathypelagic waters (Fig. 1c). Hence, AOA are apparently only abundant throughout the water column in the northern North Atlantic with its newly formed and therefore, young deep waters[23,25,26]. The major fraction of the abundant *Crenarchaeota* in the subtropical and tropical North Atlantic deep waters most likely use energy sources other than ammonia.

To assess the diversity of AOA in the meso- and bathypelagic waters of the North Atlantic, archaeal *amo*A clone libraries were established for two mesopelagic samples where Q-PCR analyses revealed relatively high numbers of AOA, and for one bathypelagic sample where the AOA abundance was very low (Supplementary Table 3). The bathypelagic clone library exhibited the lowest observed and estimated operational taxonomic units (OTUs) richness (Supplementary Fig. 3 and Table 4). The richness levels of the two mesopelagic clone libraries were comparable or higher than those observed for archaeal *amo*A clone libraries from other marine pelagic environments[11] (Supplementary Table 4). In a DNA-based phylogenetic tree, the obtained sequences fell into two distinct groups: cluster A or "shallow" cluster and cluster B or "deep" cluster[5,11,27] (Fig. 2). Based on phylogenetic analyses of PCR clone libraries, individual regions of the mesopelagic North Atlantic harbour specific archaeal *amo*A sequences (i.e., North Atlantic and equatorial subclusters, Fig. 2). More than half of the sequences of the clone library from the mesopelagic North Atlantic formed a coherent cluster closely related to sequences obtained from the same region[3]. Similarly, specific sequences recovered from the bathypelagic clone library fell into the bathypelagic subcluster 1 within cluster A and into the bathypelagic subcluster 2 of the phylogenetically distinct cluster B (Fig. 2). About 60% of the obtained archaeal *amo*A sequences were affiliated to the North Atlantic

subcluster harbouring *amo*A sequences from a diverse range of marine habitats[3-5,11,22] (Fig. 2). Taken together, our phylogenetic analyses indicate latitudinal and vertical differences among archaeal *amo*A sequences with generally rather low diversity in equatorial bathypelagic waters (Supplementary Fig. 3) coinciding with the rather low abundance of AOA. There is, however, still the possibility that deep ocean *Crenarchaeota* harbour specific versions of *amo*A genes not targeted by the thus far available primer sets.

An archaeal 16S rRNA clone library was also established for one mesopelagic sample and 3 bathypelagic samples (for details see Supplementary information). In a DNA-based phylogenetic tree, the obtained crenarchaeal sequences fell into the MCGI and pSL12-like groups (Supplementary Fig. 4). The phylogenetic analyses of the archaeal 16S rRNA genes strengthen also the idea that specific water masses harbour specific ecotypes and that the presence of OTU 2, closely related to *Nitrosopumilus maritimus*, especially in the TRANSAT sample might explain the high abundance of *amo*A genes in this specific water mass (for details see Supplementary information).

Ammonia oxidizing Archaea are generally chemoautotrophic using acetyl-coenzyme A carboxylase to fix inorganic carbon[28]. Hence, if AOA are the dominating nitrifiers as suggested by the much higher archaeal than bacterial *amo*A copy numbers, one would expect a tight relation between archaeal *amo*A copy numbers and bulk CO_2 fixation rates. Relating the dark CO_2 fixation rates obtained at these specific stations and depths by Herndl *et al.*[8] and Reinthaler and Herndl (unpublished) to the archaeal *amo*A copy numbers determined in this study, it appears that about 50% of the variation in CO_2 fixation rates can be explained by archaeal *amo*A abundance (Fig. 3). This provides further independent evidence that the vast majority of the bathypelagic *Crenarchaeota* are not chemoautotrophic nitrifiers but most likely use organic substrate as carbon and energy source as indicated also by

microautoradiography combined with fluorescence in situ hybridization and genomic analyses[8,16-18,21,27]. This conclusion is further supported by recent comparative metagenomic analyses of uncultivated Archaea of various meso- and bathypelagic oceanic regions by Martin-Cuadrado *et al.*[29]. In none of the nine fosmid libraries of MCGI from 500 m to 3000 m depth, *amo*A genes were detected[29].

In summary, it appears that only in the northern part of the North Atlantic mesophilic Archaea are predominantly oxidizing ammonia as an energy source throughout the water column including the bathypelagic realm. The abundance of putatively ammonia oxidizing Crenarchaeota gradually decreases in the meso- and bathypelagic waters from the north to the equator in the Atlantic coinciding with an increasing age of these water masses and concomitantly, a decrease in the diversity of archaeal *amo*A sequences. In the subtropical and equatorial bathypelagic waters, AOA contribute less than 1 % to the crenarchaeal community. Hence, only a minor fraction of the bathypelagic marine *Crenarchaeota* is putatively oxidizing ammonia in the temperate and subtropical North Atlantic. Consequently, a heterotrophic life mode of bathypelagic *Crenarchaeota* seems to become increasingly important from north to south in the Atlantic's interior.

Methods summary

Sampling was conducted aboard RV Pelagia during two cruises (TRANSAT-1 and ARCHIMEDES-2) following the North Atlantic Deep Water from 65°N to 5°S in the eastern basin of the Atlantic Ocean. Specific water masses were identified and sampled based on their physical and chemical characteristics.

Using quantitative PCR, the copy numbers of MCGI 16S rRNA, pSL12-like 16S rRNA, archaeal *amo*A and β-proteobacterial *amo*A genes were determined using specific primers and SYBRGreen.

Archaeal *amo*A clone libraries were generated from two stations: Station A33 at 2 distinct depths (749 m and 2502 m) and Station T28 at 597 m depth by PCR amplification using specific archaeal *amo*A primers. Archaeal 16S rRNA gene clone libraries were generated from 3 stations: Station T9 at 2071 m, Station A3 at 2 distinct depths (249 m and 2750 m) and one additional station in the Romanche Fracture Zone (-0.21°N, -18.43°E) near the station A33 (1°N, -20.60°E) at 7155 m depth by PCR amplification using specific archaeal primers.

Dark archaeal CO_2 fixation was measured via the incorporation of [^{14}C]-bicarbonate. The resulting mean disintegrations per minute (DPM) of the samples were converted into organic carbon produced over time and corrected for the natural dissolved inorganic carbon (DIC) concentration.

Supplementary information is linked to the online version of the paper at www.nature.com/nature.

Authors contributions The manuscript was written by H.A. and G.J.H. DNA extractions were performed by H.A. and M.B., quantitative PCR by H.A., M.B. and J.D. and phylogenetic analyses by M.B. DIC incorporation measurements were done by G.J.H.

Author information The archaeal sequences reported in this study have been deposited at GenBank (NCBI) under accession numbers EU650236-EU650270 (Station 3, ARCHIMEDES-2), FJ002858-FJ002876 (Station 23, ARCHIMEDES-3), FJ150794-FJ150834 (Station 9, TRANSAT-1) for 16S rRNA genes and EU795424-EU795460 and EU810209-810235 for *amo*A genes. Reprints and permissions information is available at www.nature.com/reprints. The authors declare no competing financial interest. Correspondence and requests for materials should be addressed to G.J.H. (herndl@nioz.nl).

1. Ward, B.B., Capone, D.G. & Zehr, J.P. What's new in the nitrogen cycle? *Oceanography* **20**, 101-109 (2007).
2. Schleper, C., Jurgens, G. & Jonuscheit, M. Genomic studies of uncultivated Archaea. *Nat. Rev. Microbiol.* **3**, 479-488 (2005).
3. Wuchter, C. *et al.* Archaeal nitrification in the ocean. *Proc. Natl. Acad. Sci. USA* **103**, 12317-12322 (2006).
4. Mincer, T.J. *et al.* Quantitative distribution of presumptive archaeal and bacterial nitrifiers in Monterey Bay and the North Pacific Subtropical Gyre. *Environ. Microbiol.* **9**, 1162-1175 (2007).
5. Beman, J.M., Popp, B.N. & Francis, C.A. Molecular and biogeochemical evidence for ammonia oxidation by marine Crenarchaeota in the Gulf of California. *ISME J.* **2**, 429-441 (2008).
6. Caffrey, J.M., Bano, N., Kalanetra, K. & Hollibaugh, J.T. Ammonia oxidation and ammonia-oxidizing bacteria and archaea from estuaries with differing histories of hypoxia. *ISME J.* **1**, 660-662 (2007).
7. Karner, M.B., DeLong, E.F. & Karl, D.M. Archaeal dominance in the mesopelagic zone of the Pacific Ocean. *Nature* **409**, 507-510 (2001).
8. Herndl, G.J. *et al.* Contribution of Archaea to total prokaryotic production in the deep Atlantic Ocean. *Appl. Environ. Microbiol.* **71**, 2303-2309 (2005).
9. Church, M.J. *et al.* Abundance and distribution of planktonic Archaea and Bacteria in the waters west of the Antarctic Peninsula. *Limnol. Oceanogr.* **48**, 1893-1902 (2003).
10. Venter, J.C. *et al.* Environmental genome shotgun sequencing of the Sargasso Sea. *Science* **304**, 66-74 (2004).
11. Francis, C.A., Roberts, K.J., Beman, J.M., Santoro, A.E. & Oakley, B.B. Ubiquity and diversity of ammonia-oxidizing archaea in water columns and sediments of the ocean. *Proc. Natl. Acad. Sci. USA* **102**, 14683-14688 (2005).
12. Konneke, M. *et al.* Isolation of an autotrophic ammonia-oxidizing marine archaeon. *Nature* **437**, 543-546 (2005).
13. Hallam, S.J. *et al.* Genomic analysis of the uncultivated marine crenarchaeote *Cenarchaeum symbiosum. Proc. Natl. Acad. Sci. USA* **103**, 18296-18301 (2006).
14. Leininger, S. *et al.* Archaea predominate among ammonia-oxidizing prokaryotes in soils. *Nature* **442**, 806-809 (2006).
15. Nakagawa, T., Mori, K., Kato, C., Takahashi, R. & Tokuyama, T. Distribution of the cold-adapted ammonia-oxidizing microorganisms in the deep-ocean of the Northeastern Japan Sea. *Microbes Environ.* **22**, 365-372 (2007).
16. Ouverney, C.C. & Fuhrman, J.A. Marine planktonic Archaea take up amino acids. *Appl. Environ. Microbiol.* **66**, 4829-4833 (2000).
17. Teira, E., van Aken, H., Veth, C. & Herndl, G.J. Archaeal uptake of enantiomeric amino acids in the meso- and bathypelagic waters of the North Atlantic. *Limnol. Oceanogr.* **51**, 60-69 (2006).
18. Kirchman, D.L., Elifantz, H., Dittel, A.I., Malmstrom, R.R. & Cottrell, M.T. Standing stocks and activity of Archaea and Bacteria in the western Arctic Ocean. *Limnol. Oceanogr.* **52**, 495-507 (2007).
19. Ingalls, A.E. *et al.* Quantifying archaeal community autotrophy in the mesopelagic ocean using natural radiocarbon. *Proc. Natl. Acad. Sci. USA* **103**, 6442-6447 (2006).

20. Teira, E., Lebaron, P., van Aken, H. & Herndl, G.J. Distribution and activity of Bacteria and Archaea in the deep water masses of the North Atlantic. *Limnol. Oceanogr.* **51**, 2131-2144 (2006).

21. Varela, M.M., van Aken, H.M., Sintes, E. & Herndl, G.J. Latitudinal trends of *Crenarchaeota* and Bacteria in the meso- and bathypelagic water masses of the Eastern North Atlantic. *Environ. Microbiol.* **10**, 110-124 (2008).

22. Lam, P. *et al.* Linking crenarchaeal and bacterial nitrification to anammox in the Black Sea. *Proc. Natl. Acad. Sci. USA* **104**, 7104-7109 (2007).

23. Rhein, M. *et al.* Labrador Sea Water: Pathways, CFC Inventory, and Formation Rates. *J. Phys. Oceanogr.* **32**, 648 (2002).

24. Hollibaugh, J.T., Bano, N. & Ducklow, H.W. Widespread distribution in polar oceans of a 16S rRNA gene sequence with affinity to *Nitrosospira*-like ammonia-oxidizing bacteria. *Appl. Environ. Microbiol.* **68**, 1478-1484 (2002).

25. Smethie, W.M. & Fine, R.A. Rates of North Atlantic Deep Water formation calculated from chlorofluorocarbon inventories. *Deep-Sea Res. I* **48**, 189-215 (2001).

26. van Aken, H.M. The hydrography of the mid-latitude northeast Atlantic Ocean: I: The deep water masses. *Deep-Sea Res. I* **47**, 757-788 (2000).

27. Hallam, S.J. *et al.* Pathways of carbon assimilation and ammonia oxidation suggested by environmental genomic analyses of marine *Crenarchaeota*. *PLoS Biol.* **4**, 520-536 (2006).

28. Berg, I.A., Kockelkorn, D., Buckel, W. & Fuchs, G. A 3-hydroxypropionate/4-hydroxybutyrate autotrophic carbon dioxide assimilation pathway in archaea. *Science* **318**, 1782-1786 (2007).

29. Martin-Cuadrado, A.-B. *et al.* Hindsight in the relative abundance, metabolic potential and genome dynamics of uncultivated marine archaea from comparative metagenomic analyses of bathypelagic plankton of different oceanic regions. *ISME J.* **2**, 865-886 (2008).

Figure Legends

Figure 1 │ Latitudinal and depth distribution of crenarchaeal 16S rRNA and archaeal *amo*A copy numbers in the eastern North Atlantic. **a, b.** Abundance of MCGI (a) and AOA (b) in the subsurface (*n*=9), mesopelagic (Meso) (*n*=24) and bathypelagic (Bathy) (*n*=22) waters. **c.** Ratio of archaeal *amo*A copies to crenarchaeal (MCGI + pSL12-like clade) 16S rRNA copies per ml of marine water (*n*=55). Bars indicate standard error.

Figure 2 │ Phylogenetic tree of archaeal *amo*A sequences recovered from the North Atlantic. Neighbor-joining bootstrap tree of long *amo*A-like nucleotide sequences to which we added our partial sequences (217 bp, EU795424-EU795460) and the sequences of Wuchter *et al.*[3] (217 bp, DQ784528-DQ784537) using the ARB parsimony tool (NA: North Atlantic). One representative of sequence group ≥99% identical is shown (in color); the number in front of the respective symbol indicates the number of clones. Database sequences are shown in black. Bootstrap values (>50%) are indicated at branch point.

Figure 3 │ Archaeal *amo*A copy numbers *vs.* CO_2 fixation. Relationship between archaeal *amo*A gene copy numbers and CO_2 fixation across all the stations and depths (except station T9) (*n*=31). Regression equation: $y=0.0063x^{0.5905}$.

METHODS

Study sites and sampling. Sampling was conducted aboard RV Pelagia during two cruises (TRANSAT-1 and ARCHIMEDES-2) following the North Atlantic Deep Water from 65°N to 5°S in the eastern basin of the Atlantic Ocean. Specific water masses were identified and sampled based on their physical and chemical characteristics (Supplementary Table 1). At each station, 6 depths were sampled with 10 l NOEX samplers mounted on a CTD (conductivity-temperature-depth) frame. Ten stations were used for quantitative PCR analysis (Supplementary Fig. 1).

DNA extraction of marine samples. Extraction of total DNA was performed using UltraClean soil DNA isolation kit and Mega soil DNA isolation (Mobio) for TRANSAT-1 and ARCHIMEDES-2 samples, respectively.

Quantitative PCR. The copy numbers of MCGI 16S rRNA, pSL12-like 16S rRNA, archaeal *amo*A and β-proteobacterial *amo*A genes were determined in triplicate on the non-diluted samples and in two different dilutions per sample using specific primers (Supplementary Table 2) and SYBRGreen. The 4 real-time approaches yielded highly reproducible standard curves with DNA of the plasmid 088exp4, the fosmid HF770_041/11, *Nitrosopumilus maritimus* and a mix of 4 β-proteobacteria, for MCGI, pSL12-like, archaeal *amo*A and β-proteobacterial *amo*A standards, respectively. All reactions were performed in duplicate for the standards and in triplicate for the samples and an average value was calculated for each sample. Two different methods were used to determine the presence of non-specific amplified products. No unspecific products were found in any of the analysis (See Supplementary Information for details).

Archaeal *amo*A clones libraries. Archaeal *amo*A clone libraries were generated from two stations: Station A33 at 2 distinct depths (749 m and 2502 m) and Station T28 at

597 m depth by PCR amplification using specific archaeal *amo*A primers (Supplementary Fig. 1, Table 2). The obtained sequences were compared with sequences from public database and analyzed using the ARB phylogenetic package (See Supplementary information for details).

Archaeal 16S rRNA gene clone libraries. Archaeal 16S rRNA gene clone libraries were generated from 3 stations: Station T9 at 2071 m, Station A3 at 2 distinct depths (249 m and 2750 m) and one additional station in the Romanche Fracture Zone (-0.21°N, -18.43°E) near the station A33 (1°N, -20.60°E) at 7155 m depth by PCR amplification using specific archaeal primers (Supplementary Fig. 1, Table 2). The obtained sequences were compared with sequences from public database and analyzed using the ARB phylogenetic package (see Supplementary information for details).

Archaeal CO$_2$ fixation. Dark CO$_2$ fixation was measured via the incorporation of [^{14}C]-bicarbonate (100 µCi, Amersham) in 40 ml samples in triplicate and triplicate formaldehyde-fixed blanks incubated in the dark at in situ temperature for 60-72 h. Subsequently, the incubations were terminated by adding formaldehyde (2 % final concentration) to the samples, filtered onto 0.2 µm filters (Millipore, polycarbonate), rinsed 3 times with 10 ml of ultrafiltered water (30 kDa molecular weight cut off) and then exposing the filters to a fume of concentrated HCl for 12 h. Thereafter, the filters were place in scintillation vials, 8 ml of scintillation cocktail (FilterCount, Canberra-Packard) added and after about 18 h, counted on board in a liquid scintillation counter (LKB Wallac). The instrument was calibrated with internal and external standards. The resulting mean disintegrations per minute (DPM) of the samples were corrected for the mean DPM of the blanks and converted into organic carbon produced over time and corrected for the natural dissolved inorganic carbon (DIC) concentration.

a MCGI 16S rRNA copies.ml^{-1}

b Archaeal *amo*A copies.ml^{-1}

c Ratio of archaeal *amo*A to Crenarchaeota (MCGI + pSL12-like)

Subsurface waters
100 - 150 m depth

Mesopelagic waters
200 – 1000 m

Bathypelagic waters
> 1000 m

Figure 1.

Figure 2.

Figure 3.

Supplementary information

Study sites and sampling.

During the TRANSAT-1 cruise (September 2002), in total 36 stations were occupied with RV Pelagia following a track from 65°N to 35°N in the eastern basin of the North Atlantic. Quantitative PCR analyses were done on 3 stations: T9, T20 and T28 (Supplementary Fig. 1). Sampling was performed with 22 10-L NOEX (no oxygen exchange) bottles mounted in a frame also holding sensors for conductivity, temperature, depth, chlorophyll fluorescence, and optical backscattering. The specific water masses were identified based on their temperature and salinity characteristics and their oxygen concentrations (Supplementary Table 1). One subsurface sample per station was taken from the lower euphotic layer at around 100 m depth. The waters below the surface thermocline (500 m depth) were formed by North Atlantic Central Water (NACW). Below, the 1000-2000 m depth layer was occupied by either Labrador Seawater (LSW; Sts T20, T28) or Antarctic Intermediate Water (AAIW, St T9). At Station 9, below the AAIW, slope water was present. At around 2000 m depth, the Iceland-Scotland Overflow Water (ISOW) was sampled at Stations T9 and T20. At Station T28, Middle Northeast Atlantic Deep Water (MNEADW) and Lower Northeast Atlantic Deep Water (LNEADW) were sampled at around 3000 m and 4000 m depth, respectively. For each depth, one liter of seawater was filtered onto 0.2 µm polycarbonate filter (Millipore) and the filters were subsequently stored at -80°C until further processing in the lab.

During the ARCHIMEDES-2 cruise (November to December 2006), a total of 20 stations was occupied with RV Pelagia following a track from 26°N to 5°S in the eastern (sub)tropical Atlantic. Quantitative PCR analyses were done at 7 stations: A3, A5, A11, A19, A28, A33 and A48 (Supplementary Fig. 1). Sampling was performed as described above for TRANSAT-1 and according to the water masses (Supplementary Table 1). One subsurface sample per station was taken from the lower euphotic layer at around 100 m depth. The waters below the surface thermocline (250 to 500 m depth) were formed by either North Atlantic Central Water (NACW; Sts. A3, A5 and A48) or South Atlantic Central Water (SACW; Sts. A19, A28, A33). The 700-900 m depth layer was occupied by the Subarctic Intermediate Water (SAIW) water at the northern stations, or the Antarctic Intermediate Water (AAIW) at the southern stations. Below the AAIW, the Upper Northeast Atlantic Deep Water (UNEADW), Middle Northeast Atlantic Deep Water (MNEADW) and Lower Northeast Atlantic Deep Water (LNEADW) is flowing southwards with cores at around 1800 m, 2500-

2750 m and 4000 m depth, respectively. For each depth, ten liters of seawater were filtered through a 0.22 μm Sterivex filter GP unit (Millipore) and 1.8 ml of lysis buffer (40 mM EDTA, 50 mM Tris-HCl, 0.75 M sucrose) was added and the filters subsequently stored at - 80°C until analysis.

Molecular analysis

DNA extraction and preparation of the Q-PCR standards. Archaeal 16S rRNA gene fragments were amplified from the plasmid 088exp4 (from the archaeal clones library) and the fosmid HF770_041|11 (obtained from T. Mincer[1]) as 16S rDNA, Marine *Crenarchaeota* Group I (MCGI) and pSL12-like standard, respectively, using the 16S specific primers (Parch519f and ARC915R)[2]. The archaeal *amo*A gene of the standard was amplified from DNA of *Nitrosopumilus maritimus* (obtained from M. Könneke[3]), using specific archaeal *amo*A primers (Supplementary Table 2). The β-proteobacterial *amo*A gene for the standard was amplified using a mix (25% each) of *Nitrosomonas europaea*, *N. eutropha*, *N. marina* and *Nitrospira briensis* using specific β-proteobacterial *amo*A primers (Supplementary Table 2).

Each amplification was performed under the following conditions: 4 min initial denaturation; 35 cycles at, 94°C for 30 s, specific annealing temperature of the primer set for 40 s (Supplementary Table S2), 72°C for 2 min, 80°C for 25 s using for 1 U of Pico Maxx high fidelity DNA polymerase (Stratagene), 10x Pico Maxx PCR buffer, 0.25 mM of each dNTP, 8 μg of BSA, 0.2 μM of primers, 3mM of $MgCl_2$ and ultra pure sterile water (Sigma). Amplification products were run on an agarose gel (1%), stained with SYBRGold® (Invitrogen), bands were isolated and purified using QuickClean 5M gel extraction kit (GenScript). Purified products were quantified using a Nanodrop® spectrophotometer and the copy numbers of the 16S rRNA genes of each QPCR standard were calculated directly from the concentration of the purified DNA. Ten-fold serial dilutions ranging from 10^7 to 10^2 copies of a known copy number of the standard were used per QPCR reaction in duplicate to generate an external quantification standard.

DNA extraction and quantitative PCR of the environmental samples.
DNA extraction. Total DNA extraction from marine samples was performed using the UltraClean soil DNA isolation kit (Mobio) for the TRANSAT-1 samples and the UltraClean

Mega soil DNA isolation kit (Mobio) followed by a DNA concentration with a Centricon unit (Millipore) for ARCHIMEDES-2 samples.

Q-PCR analysis. All Q-PCR analyses were performed on an iCycler iQ 5 thermocycler (Bio-rad) equipped with i-Cycler iQ software (version 3.1, Bio-Rad). The copy numbers of MCGI 16S rDNA, pSL12-like 16S rDNA, archaeal *amo*A and β-proteobacterial *amo*A in all environmental samples were determined in triplicate on the non-diluted sample and for two different dilutions of the sample (5 times and 25 times diluted). The reaction mixture (20 µl) contained 1 U of Pico Maxx high fidelity DNA polymerase (Stratagene), 2 µl of 10x Pico Maxx PCR buffer, 0.25 mM of each dNTP, 8 µg of BSA, 0.2 µM of primers, 50 000 times diluted SYBR Green® (Invitrogen) (optimized concentration), a final concentration of 10 nM of fluorescein, 3mM of $MgCl_2$ and ultra pure sterile water (Sigma)[4]. All reactions were performed in a 96-well QPCR plates (Bio-Rad) with optical tape (Bio-Rad). One µL of diluted or non-diluted environmental DNA was added to 19 µL of mix in each well. Accumulation of newly amplified double stranded gene products was followed online as the increase of fluorescence due to the binding of the fluorescent dyes SYBRGreen® and fluorescein. Specificity for QPCR reaction was tested on agarose gel electrophoresis and with a melting curve analysis (60°C-94°C) in order to identify unspecific PCR products such as primer dimers or fragments with unexpected fragment lengths. PCR efficiencies and correlation coefficients for standard curves were as follows: for the MCGI 16S rDNA assay, 87.9-105.8% and r² = 0.991-0.999, for the pSL12-like 16S rDNA assay, 94.7-110.5% and r² = 0.949-0.999, for the archaeal *amo*A assay, 86.5-97% and r² = 0.983-0.999 and for the β-proteobacterial *amo*A assay, 77.8-88.3% and r² = 0.989-0.999. Each gene fragment was detected using a standard for the specific quantification of MCGI 16S rRNA, pSL12-like 16S rRNA, archaeal *amo*A and β-proteobacterial *amo*A genes and primer combinations and annealing temperature as listed in Table 3. Thermocycling was performed as follows: initial denaturation at 95°C for 4 min; amplification: 41 cycles at, 95°C for 30 s, primer annealing temperature for 40 s, and extension at 72°C for 30 s, 80°C for 25 s, with a plate read between each cycle; melting curve 60 – 94°C with a read every 0.5°C held for 1 s between each read.

***Amo*A gene amplification, sequencing and phylogenetic analysis of archaeal *amo*A sequences.** Archaeal *amo*A sequences were amplified with the primers Arch-*amo*A-for and Arch-*amo*A-rev (Supplementary Table 2) as described in the Q-PCR section and 35 cycles of amplification. AOA *amo*A PCR were purified (QuickClean 5M PCR purification Kit,

GenScript) and cloned into the pCR4-TOPO® vector for sequencing (Invitrogen) according to manufacturers instructions. Clones were checked for the right insert by PCR and sequencing was performed (Eurofins MWG GmbH, Germany). Sequence data were compiled using ARB software[5] and aligned with complete length sequences of closest relatives obtained from NCBI database. Using ARB, the phylogenetic tree was first generated with the aligned, almost complete length sequences of closest relatives from the NCBI data base using the neighbor-joining method. Then the short-aligned sequences were added to the tree using the ARB parsimony option.

To compare the archaeal *amo*A-based richness within each clone library, rarefaction analysis and Chao1 non parametric richness estimations were performed by using DOTUR[6]. Operational taxonomic units (OTUs) were defined as sequence group in which sequences differed by ≤ 2% (Supplementary Fig. 3 and Table 4).

Archaeal 16S rRNA gene amplification, sequencing and phylogenetic analysis of archaeal 16S rRNA sequences.

Archaeal 16S rRNA gene clone libraries were generated from 3 stations: Station T9 at 2071 m, Station A3 at 2 distinct depths (249 m and 2750 m) and one station (ARCHIMEDES-3 cruise, 0.21°N, -18.43°E) close to the station A33 (1°N, -20.60°E) at 7155 m depth by PCR amplification using a forward primer specific for Archaea and a reverse universal primer (Arch21f, 1492r)[7] (Supplementary Table 3). The 16S rDNA cloning was performed as described above. Seventy-seven, 90, 97 and 80 archaeal clones from the stations T9 at 2071 m, A3 at 249 m, A3 at 2750 m, and A33 at 7155 m, respectively, were sequenced. Among these clones, 44 (57%), 50 (56%), 83 (86%) and 32 (40%) clones from the stations T9 at 2071 m, A3 at 249 m, A3 at 2750 m, and A33 at 7155 m, respectively, were affiliated to the crenarchaeal group. A DOTUR analysis was performed on the 219 crenarchaeal sequences, 19 different OTUs were defined as sequence groups in which sequences differed by ≤ 3%. The sequences were compared with sequences from public database and analyzed using the ARB phylogenetic package (Supplementary Fig. 4).

Primers specificity.

16S rRNA genes primers. To test whether groups not targeted by our MCGI and pSL12 primers might be responsible for the observed Q-PCR pattern, archaeal 16S rRNA gene fragments were amplified, cloned, screened and sequenced (see above). Using the ARB

phylogenetic package[5], the specificity of the primers was tested on our MCGI and pSL12-clade affiliated sequences from the four archaeal clone libraries. The primers used in our quantitative PCR approach for detecting MCGI and the pSL12-like cluster targeted all the obtained sequences (data not shown). The specificity of the primers used by Mincer *et al.*[1] was also tested in silico on our MCGI sequences. These primers targeted also all the MCGI sequences (data not shown).

***Amo*A genes primers.** To test whether groups of archaeal *amo*A sequences not targeted by the archaeal *amo*A primers used in this study[8] might be responsible for the observed Q-PCR pattern, we established two clone libraries with the primers used by Mincer *et al.*[1] and Francis *et al.*[9]. These two clone libraries were established from the same bathypelagic sample as used with our primers (Station A33, 2502 m depth).

From the 45 short sequences (only 85 bp) recovered from the clone library with the Mincer *et al.*[1] set of primers, only 2 sequences fell into cluster A, all the other sequences affiliated with cluster B (data not shown). The relatively short sequences of the *amo*A gene amplified by these primers do not allow phylogenetic analyses. Mincer and coauthors used this set of primers to determine the abundance of archaeal *amo*A genes by Q-PCR. The short fragment amplified by these primers is at the end of the *amo*A gene and is not or not entirely recovered by the primers used by Wuchter *et al.*[8] and Francis *et al.*[9].

Using the primers of Francis *et al.*, we recovered 38 *amo*A sequences with a length of 595 bp affiliating exclusively to cluster B (Supplementary Fig. 5). Half of these sequences are closely related to the bathypelagic subcluster 2. The sequences belonging to cluster A recovered in our North Atlantic clone library are not detected by this set of primers. Using this set of primers for Q-PCR analysis in North Atlantic waters would underestimate the number of AOA. Hence, the archaeal *amo*A primers used in our study provide a better coverage of the entire group of marine archaeal *amo*A sequences (clusters A and B, Fig. 2), however, do not recover some subclusters within cluster B which are covered by the primers of Francis *et al.*[9] (Supplementary Fig. 5). Recently, Beman *et al.*[10] designed two new forward primers, Arch-amoAFA and Arch-amoAFB, able to amplify specifically cluster A and B of AOA, respectively. The long and closest neighbor sequences of our North Atlantic sequences (cluster A and B) are recovered in silico by these primers (Fig. 2: EF414272, EU049823, EU049824, EU049846, AB373359, EU049842, AM901414 and AB305361). Thus, we conclude that our sequences would also be recovered by the set of primers of Beman *et al.*[10].

Supplementary Figures

Supplementary Figure S1: Location of the stations where samples for quantitative PCR were taken during the TRANSAT-1 (T) and ARCHIMEDES-2 (A) cruise in the North Atlantic.

Supplementary Figure S2: Relationship between archaeal *amo*A gene copies and crenarchaeal 16S rRNA gene copies across all the stations and depths (n=55).

Supplementary Figure S3: Rarefaction curves indicating archaeal *amo*A richness within clone libraries. OTUs were defined as group of sequences differing by ≤2% at the DNA level.

Supplementary Figure S4: Phylogenetic analyses of crenarchaeal 16s rRNA recovered from the North Atlantic Ocean at different stations and depths. Neighbor-joining bootstrap tree of entire 16S rDNA sequences (including the ones of this study) to which we added partial sequence using the ARB parsimony tool. Only one representative of sequence group ≥97% identical is shown; additional symbols show the total number of clones represented by a sequence. Database sequences are given in black. Bootstrap values (>50%) are indicated at branch point.

Supplementary Figure S5: Phylogenetic tree of *amo*A sequences recovered from the bathypelagic zone at Station A33 with the set of primers used in this study (in blue) and the primers of Francis *et al.*[9] (in brown). Neighbor-joining bootstrap tree of long *amo*A-like nucleotide sequences (including the sequences recovered with the primers of Francis *et al.*[9] EU810209-EU810232) to which we added our partial sequences (217 bp, EU795424-EU795460, EU810233-EU810235) and the sequences of Wuchter *et al.*[8] (217 bp, DQ784528-DQ784537) using the ARB parsimony tool. One representative of sequence group ≥99% identical is shown; additional symbols show the total number of clones represented by a sequence. Database sequences are shown in black. Bootstrap values (>50%) are indicated at branch point.

6

Table S1: Characteristics of the water masses sampled during the TRANSAT-1 and ARCHIMEDES-2 cruise based on CTD[a] profiles at the stations (Archaeal *amo*A cloning and archaeal 16S rRNA gene cloning were performed at stations in bold and italic, respectively).

Cruise	Station	Latitude (°N)	Longitude (°E)	Depth (m)	Water mass	Temp	Salinity	Pot temp	Density	CTD oxy	AOU
TRANSAT-1	*9*	*61.63*	*-20.82*	*2071*	*ISOW*	*2.571*	*34.983*	*2.416*	*27.924*	*292.3*	*36.100*
TRANSAT-1	9	61.63	-20.82	1633	slope water	3.390	34.952	3.263	27.822	287.4	34.200
TRANSAT-1	9	61.63	-20.82	1014	AAIW	5.644	35.065	5.552	27.660	247.8	56.100
TRANSAT-1	9	61.63	-20.82	498	NACW	7.877	35.196	7.825	27.455	265.9	22.100
TRANSAT-1	9	61.63	-20.82	99	Subsurface	9.100	35.228	9.089	27.283	264.2	15.800
TRANSAT-1	20	55.91	-32.21	2500	ISOW	2.942	34.974	2.739	27.888	284.0	41.795
TRANSAT-1	20	55.91	-32.21	1897	ISOW	3.184	34.972	3.035	27.860	284.9	38.444
TRANSAT-1	20	55.91	-32.21	1147	LSW	3.757	34.915	3.669	27.753	278.8	39.707
TRANSAT-1	20	55.91	-32.21	450	NACW	6.257	35.048	6.216	27.563	237.4	61.839
TRANSAT-1	20	55.91	-32.21	149	Subsurface	7.508	34.938	7.493	27.301	264.2	26.546
TRANSAT-1	28	49.73	-26.13	3878	LNEADW	2.707	34.928	2.359	27.884	253.0	76.054
TRANSAT-1	28	49.73	-26.13	2999	MNEADW	2.873	34.943	2.620	27.874	269.8	56.977
TRANSAT-1	28	49.73	-26.13	1897	LSW	3.233	34.888	3.084	27.788	286.7	36.515
TRANSAT-1	**28**	**49.73**	**-26.13**	**597**	**NACW**	**5.701**	**34.946**	**5.649**	**27.555**	**225.6**	**77.905**
TRANSAT-1	28	49.73	-26.13	146	Subsurface	11.214	35.439	11.196	27.082	240.7	26.282
ARCHIMEDES-2	*3*	*24.50*	*-18.69*	*2750*	*MNEADW*	*2.920*	*34.952*	*2.697*	*27.875*	*230.9*	*95.237*
ARCHIMEDES-2	3	24.50	-18.69	800	SAIW	8.342	35.188	8.256	27.383	117.1	168.165
ARCHIMEDES-2	3	24.50	-18.69	499	NACW	11.824	35.603	11.758	27.105	145.1	118.393
ARCHIMEDES-2	*3*	*24.50*	*-18.69*	*249*	*NACW*	*15.902*	*36.259*	*15.862*	*26.749*	*183.9*	*57.515*
ARCHIMEDES-2	3	24.50	-18.69	99	Subsurface	19.751	36.898	19.732	26.282	216.1	7.355
ARCHIMEDES-2	5	21.32	-20.87	4001	LNEADW	2.368	34.897	2.023	27.888	244.3	87.562
ARCHIMEDES-2	5	21.32	-20.87	2748	MNEADW	2.954	34.956	2.730	27.874	234.3	91.597
ARCHIMEDES-2	5	21.32	-20.87	899	SAIW	7.069	35.045	6.980	27.457	126.8	167.168
ARCHIMEDES-2	5	21.32	-20.87	501	NACW	11.371	35.506	11.306	27.114	109.4	156.863
ARCHIMEDES-2	5	21.32	-20.87	249	NACW	13.821	35.763	13.785	26.823	92.3	160.108
ARCHIMEDES-2	5	21.32	-20.87	100	Subsurface	15.642	35.869	15.627	26.503	56.7	186.391
ARCHIMEDES-2	11	11.98	-20.21	3999	LNEADW	2.365	34.894	2.020	27.886	242.2	89.782
ARCHIMEDES-2	11	11.98	-20.21	2751	MNEADW	2.859	34.938	2.636	27.869	237.5	89.244
ARCHIMEDES-2	11	11.98	-20.21	900	transitional IW	5.993	34.778	5.912	27.389	105.0	196.989
ARCHIMEDES-2	11	11.98	-20.21	499	transitional CW	9.680	35.076	9.622	27.076	44.0	232.912

ARCHIMEDES-2	11	11.98	-20.21	250	transitional CW	12.101	35.207	12.068	26.738	86.5	176.013
ARCHIMEDES-2	11	11.98	-20.21	100	Subsurface	14.206	35.446	14.192	26.492	73.9	177.046
ARCHIMEDES-2	19	4.90	-15.19	4001	LNEADW	2.368	34.892	2.023	27.883	239.1	92.827
ARCHIMEDES-2	19	4.90	-15.19	2751	MNEADW	2.787	34.926	2.566	27.865	236.0	91.279
ARCHIMEDES-2	19	4.90	-15.19	900	AAIW	5.117	34.629	5.041	27.377	127.1	181.609
ARCHIMEDES-2	19	4.90	-15.19	500	SACW	7.938	34.758	7.887	27.101	86.9	201.628
ARCHIMEDES-2	19	4.90	-15.19	251	SACW	13.183	35.314	13.148	26.607	79.0	177.496
ARCHIMEDES-2	19	4.90	-15.19	100	Subsurface	16.219	35.655	16.203	26.205	86.2	154.580
ARCHIMEDES-2	28	-3.39	-14.83	2501	MNEADW	2.948	34.925	2.749	27.848	239.8	85.957
ARCHIMEDES-2	28	-3.39	-14.83	1799	UNEADW	3.781	34.971	3.635	27.801	240.3	78.298
ARCHIMEDES-2	28	-3.39	-14.83	901	AAIW	4.419	34.543	4.349	27.386	149.8	164.233
ARCHIMEDES-2	28	-3.39	-14.83	498	SACW	7.499	34.658	7.450	27.086	108.2	183.404
ARCHIMEDES-2	28	-3.39	-14.83	252	SACW	11.901	35.139	11.868	26.723	94.9	168.898
ARCHIMEDES-2	28	-3.39	-14.83	100	Subsurface	16.398	35.689	16.382	26.190	109.6	130.293
ARCHIMEDES-3	*23*	*-0.21*	*-18.43*	*7155*	*AABW*	*1.4212*	*34.752*	*0.700*	*27.870*	*222.4*	*121.400*
ARCHIMEDES-2	**33**	**1.00**	**-20.60**	**2502**	**MNEADW**	**2.962**	**34.934**	**2.762**	**27.855**	**245.0**	**80.673**
ARCHIMEDES-2	33	1.00	-20.60	1800	UNEADW	3.900	34.982	3.753	27.798	244.8	72.817
ARCHIMEDES-2	**33**	**1.00**	**-20.60**	**749**	**AAIW**	**5.307**	**34.513**	**5.244**	**27.260**	**142.9**	**164.551**
ARCHIMEDES-2	33	1.00	-20.60	498	SACW	7.195	34.637	7.147	27.112	127.5	166.187
ARCHIMEDES-2	33	1.00	-20.60	250	SACW	11.987	35.150	11.955	26.715	103.3	160.023
ARCHIMEDES-2	33	1.00	-20.60	99	Subsurface	16.469	35.666	16.453	26.156	117.0	122.601
ARCHIMEDES-2	48	19.19	-25.24	2500	MNEADW	3.196	34.963	2.993	27.857	234.4	89.284
ARCHIMEDES-2	48	19.19	-25.24	1798	UNEADW	4.091	35.007	3.942	27.798	212.3	103.796
ARCHIMEDES-2	48	19.19	-25.24	901	SAIW	6.707	34.939	6.621	27.423	115.5	181.197
ARCHIMEDES-2	48	19.19	-25.24	499	NACW	10.193	35.245	10.133	27.121	64.0	209.541
ARCHIMEDES-2	48	19.19	-25.24	249	NACW	13.918	35.735	13.881	26.781	83.5	168.521
ARCHIMEDES-2	48	19.19	-25.24	99	Subsurface	18.733	36.508	18.716	26.248	137.5	90.726

[a] : CTD, conductivity, temperature, depth

Water masses: NACW, North Atlantic Central Water ; SACW, South Atlantic Central Water ; transitional CW, transitional Central Water ; LSW, Labrador Sea Water ; ISOW, Iceland-Scotland Overflow Water ; SAIW, Subarctic Intermediate Water ; AAIW, Antarctic Intermediate Water ; transitional IW, transitional intermediate water ; UNEADW, Upper North East Atlantic Deep Water ; MNEADW, Middle North East Atlantic Deep Water ; LNEADW, Lower North East Atlantic Deep Water, AABW, Antarctic Bottom Water.

Parameters: temp, temperature (°C) measured with the CTD rosette ; salinity, salinity (pss) measured with the CTD rosette, pot temp, potential temperature (°C) ; density, potential density anomaly (kg.m^{-3}) ; CTD oxy, oxygen concentration (μmol.kg^{-1}) measured with the CTD rosette ; AOU, apparent oxygen utilization (μmol.kg^{-1}).

Table S2 – Primers used for detection and quantification of archaeal 16S rRNA and *amo*A genes and bacterial *amo*A genes

Target	Gene	Name	Fragment length (bp)	Annealing temperature (°C)	Sequence (5' to 3')	Reference
Marine *Crenarchaeota*	16S rRNA	MCGI-391f	122	61.0	AAGGTTARTCCGAGTGRTTTC	[8]
	16S rRNA	MCGI-554r			TGACCACTTGAGGTGCTG	[8]
pSL12-like clade	16S rRNA	pSL12_750F	326	65.0	GGTCCRCCAGAACGCGC	[1]
	16S rRNA	pSL12_876R			GTACTCCCCAGGCGGCAA	[1]
Archaeal *amo*A	*amo*A	Arch-*amo*A-for	256	58.5	CTGAYTGGGCYTGGACATC	[8]
	*amo*A	Arch-*amo*A-rev			TTCTTCTTTGTTGCCCAGTA	[8]
β- proteobacterial *amo*A	*amo*A	*amo*A-1F	490	61.5	GGGGTTTCTACTGGTGGT	[11]
	*amo*A	*amo*A-r NEW			CCCCTCBGSAAAVCCTTCTTC	[12]

Table S3: Archaeal 16S rRNA and *amo*A gene, and β-proteobacterial *amo*A gene copy numbers in the samples from the Atlantic Ocean

Cruise	Station	Depth (m)	MCGI 16S rDNA copies ml^{-1} MW (S.D.)	pSL12-like 16S rDNA copies ml^{-1} MW (s.d.)	Archaeal *amo*A gene copies ml^{-1} MW (s.d.)	β-proteobacterial *amo*A gene copies ml^{-1} MW (s.d.)
TRANSAT-1	9	2071	7.84×10^4 (7.50×10^3)	9.33×10^2 (7.52×10^1)	2.36×10^3 (5.06×10^2)	2.21×10^2 (5.13×10^1)
TRANSAT-1	9	1633	1.39×10^4 (1.83×10^3)	8.70×10^2 (2.63×10^2)	4.98×10^2 (2.52×10^1)	7.20×10^1 (1.88×10^1)
TRANSAT-1	9	1014	1.35×10^5 (4.01×10^4)	3.74×10^3 (1.20×10^3)	2.39×10^3 (3.87×10^2)	6.28×10^1 (1.74×10^1)
TRANSAT-1	9	498	3.99×10^4 (1.68×10^4)	1.81×10^3 (3.07×10^2)	4.68×10^3 (1.23×10^3)	1.75×10^2 (5.55×10^1)
TRANSAT-1	9	99	6.31×10^4 (1.09×10^4)	1.19×10^2 (1.18×10^1)	7.08×10^3 (1.98×10^3)	1.99×10^3 (7.19×10^2)
TRANSAT-1	20	2500	7.53×10^2 (1.65×10^2)	9.51×10^2 (8.07×10^1)	3.47×10^2 (2.02×10^1)	1.97×10^1 (2.90×10^0)
TRANSAT-1	20	1897	1.12×10^3 (1.25×10^2)	3.69×10^2 (5.48×10^1)	4.48×10^2 (1.93×10^2)	9.98×10^0 (-)
TRANSAT-1	20	1147	1.36×10^3 (1.71×10^2)	2.82×10^2 (1.07×10^2)	1.38×10^2 (4.28×10^1)	n.d.
TRANSAT-1	20	450	7.34×10^3 (3.02×10^3)	5.89×10^2 (1.20×10^2)	3.56×10^3 (1.11×10^3)	1.60×10^1 (-)
TRANSAT-1	20	149	8.87×10^3 (2.18×10^3)	3.78×10^2 (7.95×10^0)	2.23×10^4 (3.90×10^3)	5.93×10^2 (1.14×10^2)
TRANSAT-1	28	3878	5.10×10^4 (1.10×10^4)	2.72×10^3 (1.17×10^3)	8.52×10^1 (7.78×10^0)	8.93×10^0 (3.28×10^0)
TRANSAT-1	28	2999	5.36×10^4 (1.44×10^4)	3.53×10^3 (1.41×10^3)	1.40×10^2 (8.25×10^0)	3.00×10^0 (4.56×10^{-1})
TRANSAT-1	28	1897	5.00×10^4 (8.02×10^3)	3.18×10^3 (-)	7.98×10^1 (1.68×10^1)	n.d.
TRANSAT-1	28	597	2.13×10^5 (4.69×10^4)	4.52×10^3 (1.53×10^3)	5.52×10^3 (1.07×10^3)	9.78×10^2 (1.61×10^1)
TRANSAT-1	28	146	1.38×10^5 (4.49×10^4)	1.45×10^3 (6.67×10^2)	9.52×10^3 (9.83×10^2)	1.33×10^2 (2.70×10^1)
ARCHIMEDES-2	3	2750	2.30×10^4 (2.03×10^3)	1.67×10^2 (1.63×10^1)	7.80×10^1 (2.96×10^1)	5.23×10^{-2} (1.54×10^{-2})
ARCHIMEDES-2	3	800	2.21×10^5 (4.93×10^4)	1.41×10^3 (5.94×10^1)	7.98×10^1 (2.18×10^1)	n.d.
ARCHIMEDES-2	3	499	2.49×10^4 (3.76×10^3)	1.10×10^3 (2.62×10^2)	1.38×10^2 (1.95×10^1)	n.d.
ARCHIMEDES-2	3	249	1.24×10^4 (9.64×10^2)	4.69×10^3 (9.04×10^2)	7.48×10^2 (2.51×10^2)	n.d.
ARCHIMEDES-2	3	99	2.60×10^3 (4.98×10^2)	2.30×10^1 (1.77×10^0)	2.49×10^3 (8.78×10^1)	8.85×10^{-2} (4.53×10^{-2})
ARCHIMEDES-2	5	4001	1.54×10^4 (2.31×10^3)	5.79×10^1 (-)	2.04×10^2 (4.90×10^1)	6.58×10^{-1} (5.23×10^{-2})
ARCHIMEDES-2	5	2748	4.01×10^3 (4.62×10^2)	6.10×10^1 (9.82×10^0)	1.51×10^1 (2.29×10^0)	6.02×10^{-2} (1.10×10^{-2})
ARCHIMEDES-2	5	899	1.39×10^4 (2.00×10^3)	1.32×10^2 (7.71×10^1)	7.68×10^1 (2.09×10^1)	9.70×10^{-1} (7.57×10^{-1})
ARCHIMEDES-2	5	501	7.16×10^4 (1.68×10^4)	2.20×10^2 (1.20×10^2)	1.59×10^3 (2.76×10^2)	9.28×10^{-1} (2.47×10^{-2})
ARCHIMEDES-2	5	249	8.37×10^5 (2.29×10^5)	6.16×10^2 (7.07×10^1)	4.73×10^3 (4.68×10^2)	2.31×10^0 (5.90×10^{-1})
ARCHIMEDES-2	5	100	1.03×10^5 (3.88×10^4)	4.85×10^2 (1.54×10^2)	2.32×10^4 (2.62×10^3)	5.94×10^1 (6.55×10^0)

ARCHIMEDES-2	11	3999	1.44×10^4 (2.78×10^3)	4.38×10^2 (2.07×10^2)	1.03×10^1 (1.73×10^0)	1.41×10^0 (7.43×10^{-1})
ARCHIMEDES-2	11	2751	2.54×10^4 (1.15×10^3)	1.92×10^2 (1.04×10^1)	3.40×10^1 (5.97×10^0)	2.56×10^0 (1.32×10^0)
ARCHIMEDES-2	11	900	1.21×10^5 (4.37×10^4)	2.13×10^2 (6.17×10^1)	3.75×10^1 (1.08×10^1)	1.33×10^1 $(-)$
ARCHIMEDES-2	11	499	1.50×10^5 (3.05×10^4)	4.95×10^2 (2.84×10^1)	1.92×10^2 (3.50×10^1)	5.30×10^1 (8.84×10^0)
ARCHIMEDES-2	11	250	4.02×10^5 (7.04×10^4)	2.29×10^3 (3.64×10^2)	2.57×10^3 (6.73×10^2)	1.13×10^2 (3.84×10^1)
ARCHIMEDES-2	11	100	2.35×10^5 (3.53×10^4)	2.87×10^2 (5.75×10^1)	2.53×10^4 (7.42×10^2)	1.87×10^1 $(-)$
ARCHIMEDES-2	19	4001	2.86×10^3 (6.52×10^2)	5.73×10^2 (1.48×10^2)	3.80×10^0 (2.28×10^0)	n.d.
ARCHIMEDES-2	19	2751	3.23×10^4 (6.54×10^3)	2.85×10^2 (1.90×10^1)	6.05×10^0 (4.95×10^{-1})	4.33×10^{-2} $(-)$
ARCHIMEDES-2	19	900	1.60×10^4 (4.98×10^3)	6.75×10^2 $(-)$	1.84×10^1 (4.62×10^0)	n.d.
ARCHIMEDES-2	19	500	2.85×10^4 (6.88×10^3)	4.80×10^2 (2.09×10^2)	1.41×10^1 $(-)$	n.d.
ARCHIMEDES-2	19	251	1.27×10^5 (5.84×10^4)	1.57×10^3 (7.26×10^2)	8.15×10^2 (1.15×10^2)	n.d.
ARCHIMEDES-2	19	100	7.09×10^4 (3.77×10^4)	1.15×10^2 (1.18×10^1)	3.32×10^4 (1.05×10^4)	n.d.
ARCHIMEDES-2	28	2501	3.31×10^4 (3.71×10^3)	3.67×10^3 (1.46×10^3)	5.54×10^1 (7.27×10^0)	1.52×10^{-1} $(-)$
ARCHIMEDES-2	28	1799	5.19×10^2 (9.93×10^1)	2.87×10^3 (5.08×10^2)	6.46×10^0 (1.20×10^0)	n.d.
ARCHIMEDES-2	28	901	8.54×10^4 (2.30×10^3)	1.12×10^3 (5.30×10^2)	1.50×10^1 (4.22×10^0)	1.27×10^{-1} (4.54×10^{-2})
ARCHIMEDES-2	28	498	3.83×10^4 (2.07×10^4)	1.83×10^3 (5.90×10^2)	1.70×10^2 (1.27×10^1)	4.36×10^{-2} (2.09×10^{-2})
ARCHIMEDES-2	28	252	4.71×10^5 (8.41×10^4)	2.08×10^4 (2.25×10^3)	2.39×10^3 (4.87×10^2)	2.34×10^{-1} (7.09×10^{-2})
ARCHIMEDES-2	28	100	1.28×10^4 (4.17×10^3)	1.38×10^2 (9.85×10^0)	1.20×10^4 (8.52×10^2)	4.31×10^{-1} (1.67×10^{-1})
ARCHIMEDES-2	33	2502	5.35×10^4 (1.36×10^4)	2.90×10^3 (6.65×10^2)	6.47×10^1 (1.88×10^1)	n.d.
ARCHIMEDES-2	33	1800	2.70×10^4 (2.12×10^3)	1.53×10^3 (2.92×10^2)	3.53×10^1 (3.69×10^0)	n.d.
ARCHIMEDES-2	33	749	4.51×10^5 (1.88×10^5)	3.61×10^3 (2.02×10^2)	1.29×10^4 (1.91×10^3)	3.95×10^{-2} $(-)$
ARCHIMEDES-2	33	498	3.24×10^5 (4.54×10^4)	1.27×10^3 (2.9×10^2)	1.39×10^2 (3.09×10^1)	3.89×10^{-2} $(-)$
ARCHIMEDES-2	33	250	3.36×10^5 (9.88×10^4)	4.84×10^3 (1.04×10^3)	2.68×10^3 (1.24×10^2)	9.82×10^{-2} (4.36×10^{-2})
ARCHIMEDES-2	33	99	3.10×10^4 (3.67×10^3)	1.56×10^3 (3.36×10^2)	2.50×10^4 (1.20×10^3)	3.19×10^{-2} $(-)$
ARCHIMEDES-2	48	2500	1.69×10^3 (1.18×10^2)	2.63×10^2 (8.87×10^1)	6.65×10^0 (7.07×10^{-2})	1.62×10^{-1} $(-)$
ARCHIMEDES-2	48	1798	7.07×10^3 (1.90×10^3)	1.27×10^2 (4.36×10^1)	6.78×10^0 (1.31×10^0)	n.d.
ARCHIMEDES-2	48	901	5.04×10^3 (2.14×10^3)	7.18×10^1 (1.06×10^0)	1.73×10^0 (1.16×10^0)	1.96×10^{-1} $(-)$
ARCHIMEDES-2	48	499	2.43×10^5 (7.20×10^4)	7.48×10^2 (3.10×10^2)	5.33×10^2 (1.08×10^2)	1.81×10^{-1} (4.08×10^{-2})
ARCHIMEDES-2	48	249	1.83×10^4 (5.20×10^3)	5.93×10^2 (1.88×10^2)	3.24×10^2 (8.53×10^1)	1.21×10^{-1} $(-)$

s.d.: standard deviation ; MW: marine water ; n.d.: not detected (i.e., no specific product formed upon Q-PCR or below detection limit).

Table S4 – Observed and estimated richness in archaeal *amo*A gene libraries

Station	Depth	Water Mass	No. of clones sequenced	No. of OTUs (2%)	Chao1 (2%)
TRANSAT-1, station 28	597 m	NACW	45	15	20
ARCHIMEDES-2, station 33	749 m	AAIW	39	8	18
ARCHIMEDES-2, station 33	2502 m	MNEADW	39	7	8.5

Supplementary notes (references)

1. Mincer, T.J. *et al.* Quantitative distribution of presumptive archaeal and bacterial nitrifiers in Monterey Bay and the North Pacific Subtropical Gyre. *Environ. Microbiol.* **9**, 1162-1175 (2007).

2. Coolen, M.J.L. *et al.* Evolution of the methane cycle in Ace Lake (Antarctica) during the Holocene: Response of methanogens and methanotrophs to environmental change. *Org. Geochem.* **35**, 1151-1167 (2004).

3. Konneke, M. *et al.* Isolation of an autotrophic ammonia-oxidizing marine archaeon. *Nature* **437**, 543-546 (2005).

4. Coolen, M.J.L. *et al.* Ancient DNA derived from alkenone-biosynthesizing haptophytes and other algae in Holocene sediments from the Black Sea. *Paleoceanography* **21**, PA1005, 1010.1029/2005PA001188 (2006).

5. Ludwig, W. *et al.* ARB: a software environment for sequence data. *Nucleic Acids Res.* **32**, 1363-1371 (2004).

6. Schloss, P.D. & Handelsman, J. Introducing DOTUR, a computer program for defining operational taxonomic units and estimating species richness. *Appl. Environ. Microbiol.* **71**, 1501-1506 (2005).

7. Delong, E.F. Archaea in coastal marine environments. *Proc. Natl. Acad. Sci. USA* **89**, 5685-5689 (1992).

8. Wuchter, C. *et al.* Archaeal nitrification in the ocean. *Proc. Natl. Acad. Sci. USA* **103**, 12317-12322 (2006).

9. Francis, C.A., Roberts, K.J., Beman, J.M., Santoro, A.E. & Oakley, B.B. Ubiquity and diversity of ammonia-oxidizing archaea in water columns and sediments of the ocean. *Proc. Natl. Acad. Sci. USA* **102**, 14683-14688 (2005).

10. Beman, J.M., Popp, B.N. & Francis, C.A. Molecular and biogeochemical evidence for ammonia oxidation by marine Crenarchaeota in the Gulf of California. *ISME J.* **2**, 429-441 (2008).

11. Rotthauwe, J.H., Witzel, K.P. & Liesack, W. The ammonia monooxygenase structural gene *amo*A as a functional marker: Molecular fine-scale analysis of natural ammonia-oxidizing populations. *Appl. Environ. Microbiol.* **63**, 4704-4712 (1997).

12. Hornek, R. *et al.* Primers containing universal bases reduce multiple *amo*A gene specific DGGE band patterns when analysing the diversity of beta-ammonia oxidizers in the environment. *J. Microbiol. Methods* **66**, 147-155 (2006).
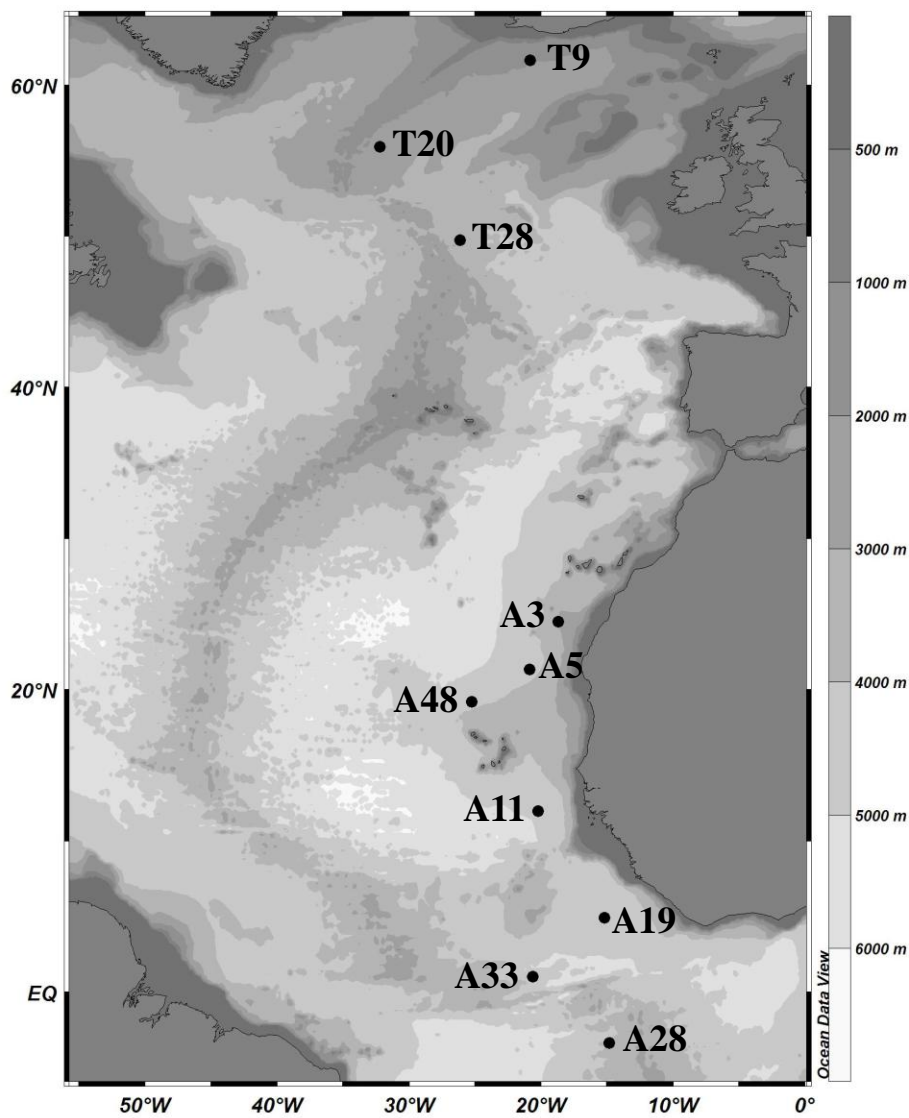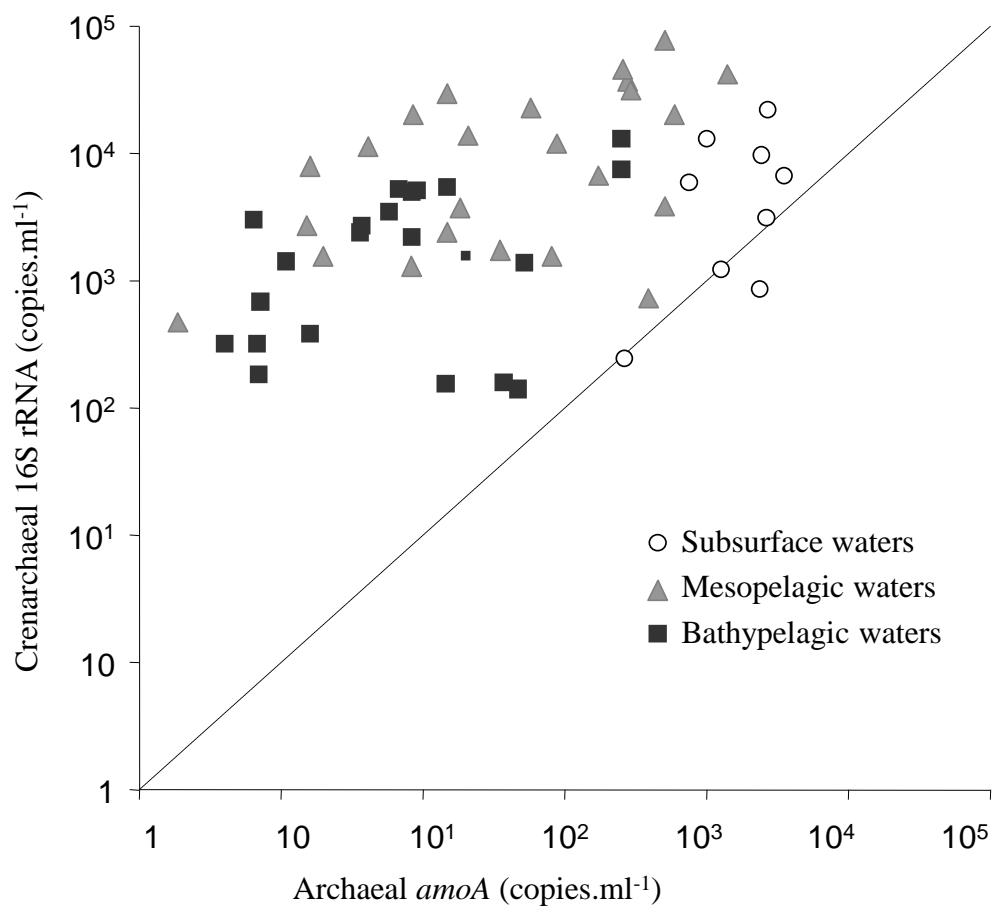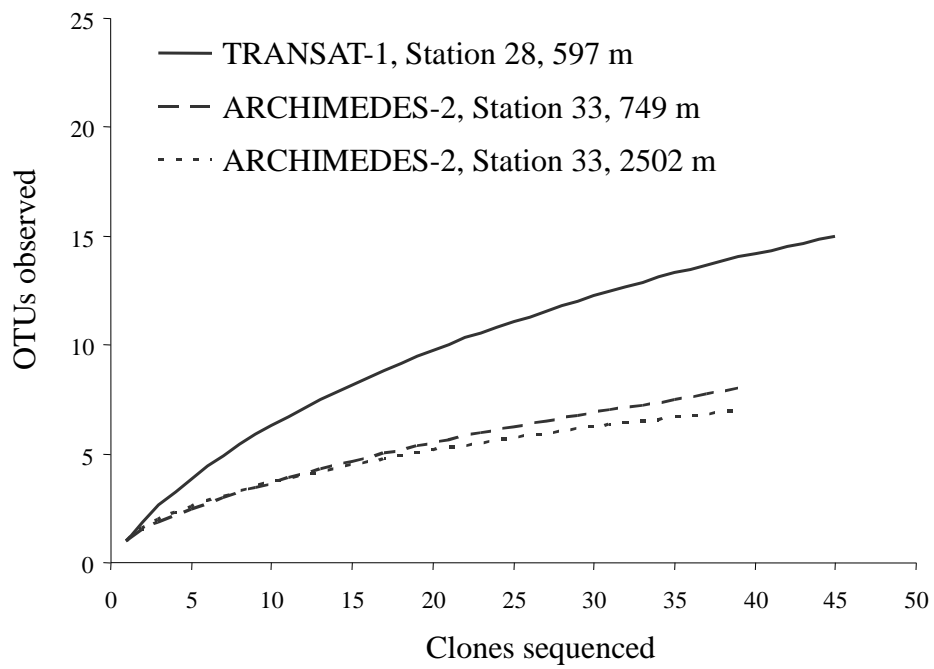
Figure S1.

Figure S2.

Figure S3.

Figure S4.

Figure S5.